



Lawrence Berkeley Laboratory

UNIVERSITY OF CALIFORNIA

RECEIVED

LAWRENCE
BERKELEY LABORATORY

APR 16 1982

LIBRARY AND
DOCUMENTS SECTION

ENERGY & ENVIRONMENT DIVISION

Presented at the International Energy Agency (IEA)
Energy Audit Workshop, Elsinore, Denmark,
April 13-15, 1981

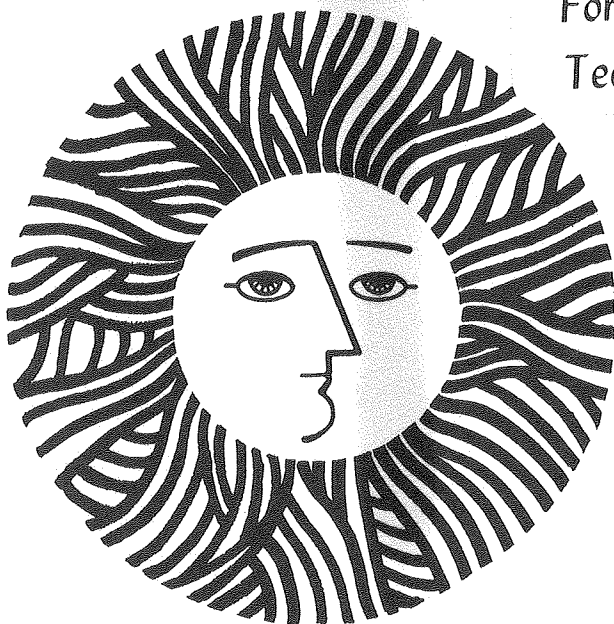
INFILTRATION MEASUREMENTS IN AUDIT AND RETROFIT
PROGRAMS

D.T. Grimsrud, R.C. Sonderegger, and M.H. Sherman

April 1981

TWO-WEEK LOAN COPY

This is a Library Circulating Copy
which may be borrowed for two weeks.
For a personal retention copy, call
Tech. Info. Division, Ext. 6782



LBL-12221
e2

DISCLAIMER

This document was prepared as an account of work sponsored by the United States Government. While this document is believed to contain correct information, neither the United States Government nor any agency thereof, nor the Regents of the University of California, nor any of their employees, makes any warranty, express or implied, or assumes any legal responsibility for the accuracy, completeness, or usefulness of any information, apparatus, product, or process disclosed, or represents that its use would not infringe privately owned rights. Reference herein to any specific commercial product, process, or service by its trade name, trademark, manufacturer, or otherwise, does not necessarily constitute or imply its endorsement, recommendation, or favoring by the United States Government or any agency thereof, or the Regents of the University of California. The views and opinions of authors expressed herein do not necessarily state or reflect those of the United States Government or any agency thereof or the Regents of the University of California.

Presented at the International Energy Agency (IEA) Energy Audit Workshop, Elsinore, Denmark, April 13-15, 1981.

INFILTRATION MEASUREMENTS IN
AUDIT AND RETROFIT PROGRAMS

D. T. Grimsrud, R.C. Sonderegger, and M.H. Sherman

Energy and Environment Division
Lawrence Berkeley Laboratory
University of California
Berkeley, CA 94720

April 1981

This work was supported by the Assistant Secretary for Conservation and Renewable Energy, Office of Buildings and Community Systems, Buildings Division, of the U.S. Department of Energy under Contract No. DE-AC03-76SF00098.

Infiltration Measurements in
Audit and Retrofit Programs

D.T. Grimsrud, R.C. Sonderegger and M.H. Sherman

Energy and Environment Division
Lawrence Berkeley Laboratory
University of California
Berkeley, CA 94720

Abstract

A model that relates fan pressurization measurements to infiltration values during the heating season is the basis for infiltration estimates in several different audit programs. We describe the model and present validation results. The model is used in three different audit strategies. The first is an energy audit to determine economically optimal retrofits for residential buildings, based on actual, on-site measurements of key indices of the house. Measurements are analyzed on a microprocessor and retrofit combinations compatible with minimum life-cycle cost and occupant preferences are determined. The second uses graphical techniques to make infiltration calculations while the third is a non-instrumented walk-through audit that was developed as a standard reference in the Residential Conservation Service Program.

Introduction

Energy conservation in buildings has been and will continue to be an important issue in the United States. The building sector alone accounts for a third of our national energy consumption. While an obvious response to this situation is to change construction practices to assure more energy efficiency in buildings, the time scale of such a shift will be long -- 80% of the 1990 housing stock in the United States has already been built.

This work was supported by the Assistant Secretary for Conservation and Renewable Energy, Office of Buildings and Community Systems, Buildings Division, of the U.S. Department of Energy under Contract No. DE-AC03-76SF00098.

Audit and retrofit programs, designed to improve the condition of existing buildings, are beginning in several areas of the country. An important part of any audit is its assessment of infiltration. This paper describes a technique to determine the infiltration of a house using simple instrumentation or estimation procedures. The model is then applied in three different residential audit designs to illustrate its wide applicability.

Infiltration

Infiltration, the uncontrolled leakage of air into a house, is a sizeable fraction of the energy load of the structure. Several standard techniques exist to measure infiltration in a building [1-3]; however, few of the standard techniques are applicable for an energy audit. Even if a measurement could be made within the time constraint of an audit, the result could be generalized to a seasonal infiltration only with great uncertainty. This has forced us to adopt a different strategy, viz., adopt either a short, cursory examination of the structure or use a less direct measurement procedure using fan pressurization. The simplicity and speed of the latter technique and the quality of the infiltration predictions obtainable with it make it a prime candidate for inclusion in the audit. If instrumentation for fan pressurization measurements is not available, another procedure, described later, is suggested.

Fan pressurization has been described in several publications [4-6]; consequently our description shall concentrate on features unique to our measurement procedure. A fan mounted on an adjustable wooden plate is sealed into a doorway of a house to be tested. The fan speed, which can be adjusted using a DC motor and controller, is varied to produce a pressure drop, ΔP , across the building envelope. The flow through the fan required to produce this pressure difference is measured and the process repeated for fixed pressure increments to produce a curve relating the pressure drop across the envelope to the flow required to produce it. The fan direction is reversed and a corresponding curve of depressurization versus flow is obtained in the same manner.

The flows at equal positive and negative pressures are averaged. In the pressure region used (± 10 to ± 60 Pa), the data generally form a straight line on a log-log plot, i.e., the data are well represented by the empirical relationship

$$Q = K \Delta P^n \quad (1)$$

where: Q is the volume flow rate of the fan [m^3/s],
 K is a constant,
 ΔP is the absolute value of the pressure drop across the building envelope [Pa], and
 n is an exponent in the range $0.5 < n < 1.0$.

The curve is then extrapolated toward the low-pressure end of the graph to determine the flow at 4 pascals. A particular flow model is now invoked to compute the effective leakage area (ELA) of the structure. An assumption is made that in the low-pressure regime in the vicinity of 4 pascals (a pressure typical of the pressures that drive natural infiltration) the pressure-flow relationship has the form of inviscid flow through large openings, i.e.

$$Q = L \sqrt{\frac{2}{\rho} \Delta P} \quad \text{for } \Delta P \approx 4 \text{ Pa} \quad (2)$$

where: L is the effective leakage area [m^2], and
 ρ is the density of air [kg/m^3].

Our choice of the form of the flow relationship given in Eq (2) is the result of measurements of the leakage of a house at very low pressures using a technique we call AC pressurization [7]. These measurements show that, even at pressures as low as a few tenths of a pascal, the flow characteristic for the houses tested was typical of the flow through an orifice (inviscid flow) rather than flow through narrow cracks dominated by viscous interactions with the walls.

A model relating the effective leakage area measured with fan pressurization to the infiltration experienced in various weather conditions has been developed at Lawrence Berkeley Laboratory [8]. The model is the key element that allows the inclusion of fan pressurization measurements in an energy audit to predict infiltration values. Briefly, the model combines the effective leakage area, L , with parameters associated with the house and the local weather conditions to predict the infiltration, Q .

$$Q = L \left[f_s^2 \Delta T + f_w^2 v^2 \right]^{1/2} \quad (3)$$

where: Q is the infiltration [m^3/s],
 L is the effective leakage area [m^2],
 ΔT is the average indoor-outdoor temperature difference [K],
 f_s is called the reduced stack parameter [$m/s/K^{1/2}$],
 v is the average wind speed at the house, and
 f_w is the reduced wind parameter.

The first term in brackets, when multiplied by the effective leakage area, represents the stack-effect component of the infiltration, the second, the wind-effect component.

Eq (3) displays the inherent simplicity of the model. The infiltration is the product of terms that depend only on the structure of the house and its surrounding terrain (L , f_w , f_s) and weather-dependent terms (ΔT , v). Once f_w , f_s and the effective leakage area are determined, the average infiltration for any particular time interval is found by determining the average values of ΔT and v for that interval and combining them by using Eq (3). Therefore, sequential predictions of infiltration only require sequential weather information, but no additional information about the house or terrain.

The terms f_s and f_w are complex expressions but their interpretations are straightforward. We must first introduce two additional expressions: the fraction of the total leakage that is horizontal (i.e., the sum of the floor and ceiling leakage areas divided by the total) is called R .

$$R = \frac{L_c + L_f}{L} \quad (4)$$

The fractional difference between the ceiling leakage area, L_c , and floor leakage area, L_f , is called X.

$$X = \frac{L_c - L_f}{L} \quad (5)$$

The stack parameter is expressed in terms of R, X, the acceleration of gravity, g, the absolute indoor temperature, T, and the height of the ceiling above grade, H_h , as:

$$f_s = \frac{1}{3} \left(1 + \frac{R}{2}\right) \left[1 - \frac{X^2}{(2 - R)^2}\right]^{3/2} \left(\frac{gH_h}{T}\right)^{1/2} \quad (6)$$

The wind pressures on the surface of the house depend upon the terrain class and the shielding class of the structure. The terrain class is affected by the large-scale obstructions in the several-square-km region of the house. The shielding class is determined by the number of trees, fences, and other buildings located in the immediate vicinity of the house.

The wind speed at a measurement site in the region is first corrected to a speed at a standard height using the terrain class at the measurement site, then is adjusted back to the wind speed at the height of the house using the terrain class of the house. Combining all the terms we have:

$$f_w = C' (1 - R)^{1/3} \left[\frac{\alpha_h (H_h/10)^{\gamma_h}}{\alpha_m (H_m/10)^{\gamma_m}} \right] \quad (7)$$

where: C' is the shielding coefficient for the house site,
 R is the fractional horizontal leakage area,
 α_h, γ_h are the terrain class constants for the house,
 H_h is the height of the house [m],
 α_m, γ_m are the terrain class constants for the wind-measurement site,
and
 H_m is the height of the wind measurement [m].

The values of α and γ for standard terrain classes are presented in Table 1, below.

Table 1: Terrain parameters for standard terrain classes			
Class	γ	α	Description
I	0.10	1.30	Ocean or other body of water with at least 5 km of unrestricted expanse
II	0.15	1.00	Flat terrain with some isolated obstacles (e.g., buildings or trees well separated from each other
III	0.20	0.85	Rural areas with low buildings, trees, etc.
IV	0.25	0.67	Urban, industrial or forest areas
V	0.35	0.47	Center of large city

Most airport wind-speed measurements are made in terrain class II while most houses are located in terrain classes III and IV. The generalized shielding coefficients are presented in Table 2, below.

Table 2: Generalized shielding coefficient vs. local shielding		
Shielding Class	C'	Description
I	0.324	No obstructions (trees, fences, nearby houses) whatsoever
II	0.285	Light local shielding with few obstructions
III	0.240	Some obstructions within two house heights
IV	0.185	Obstructions around most of perimeter
V	0.102	Large obstruction surrounding perimeter within two house heights

Examples of the ability of the model to predict infiltration on a short-term basis are shown in Fig.1 and 2. Here, we show two separate three-day data sets recently measured by our Mobile Infiltration Test Unit (MITU), a trailer equipped with adjustable leaks and cracks, pressure sensors and weather station used for detailed field investigations of air infiltration phenomena. The solid lines show infiltration measurements obtained using a controlled-flow injection system [3] at half-hour intervals over the three-day periods shown. The dotted lines represent the infiltration predicted for this structure using Eq (3).

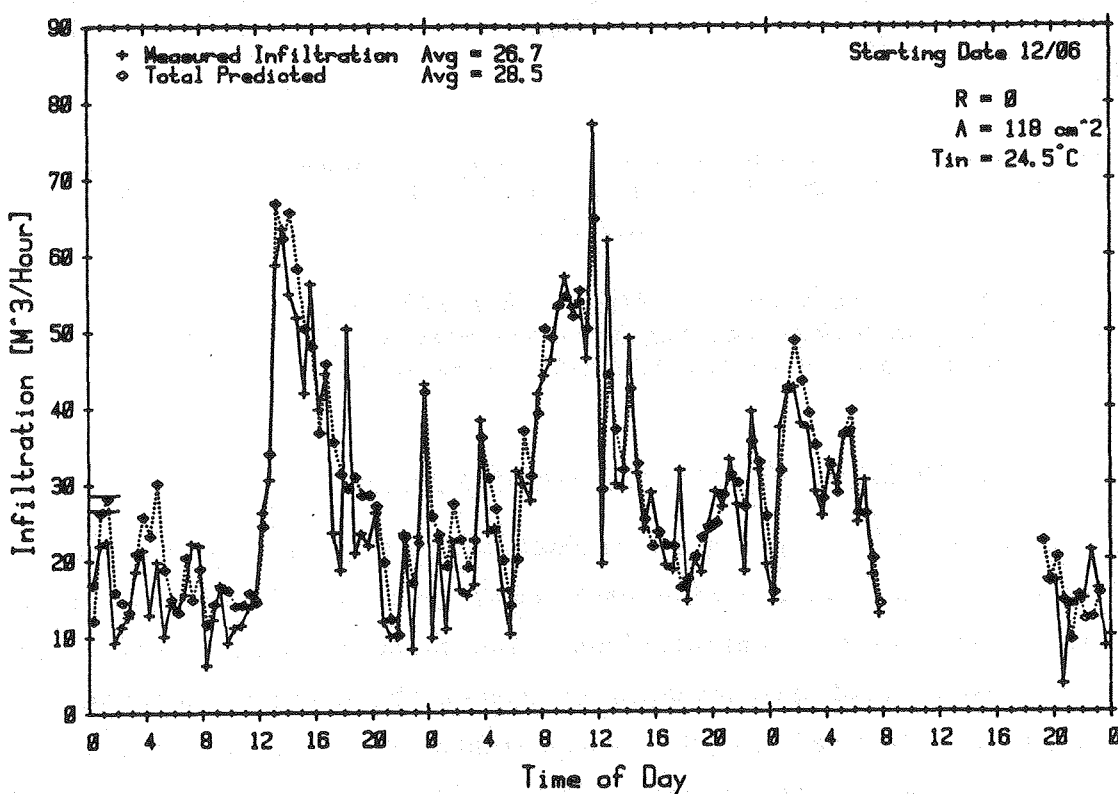


Fig.1 Air Infiltration vs. Time 80/12/06 - 80/12/08. The solid line shows measured infiltration values; the dotted line shows values predicted for the MITU using Eq (3). One ach is equivalent to $29 \text{ m}^3/\text{hr}$ in this structure.

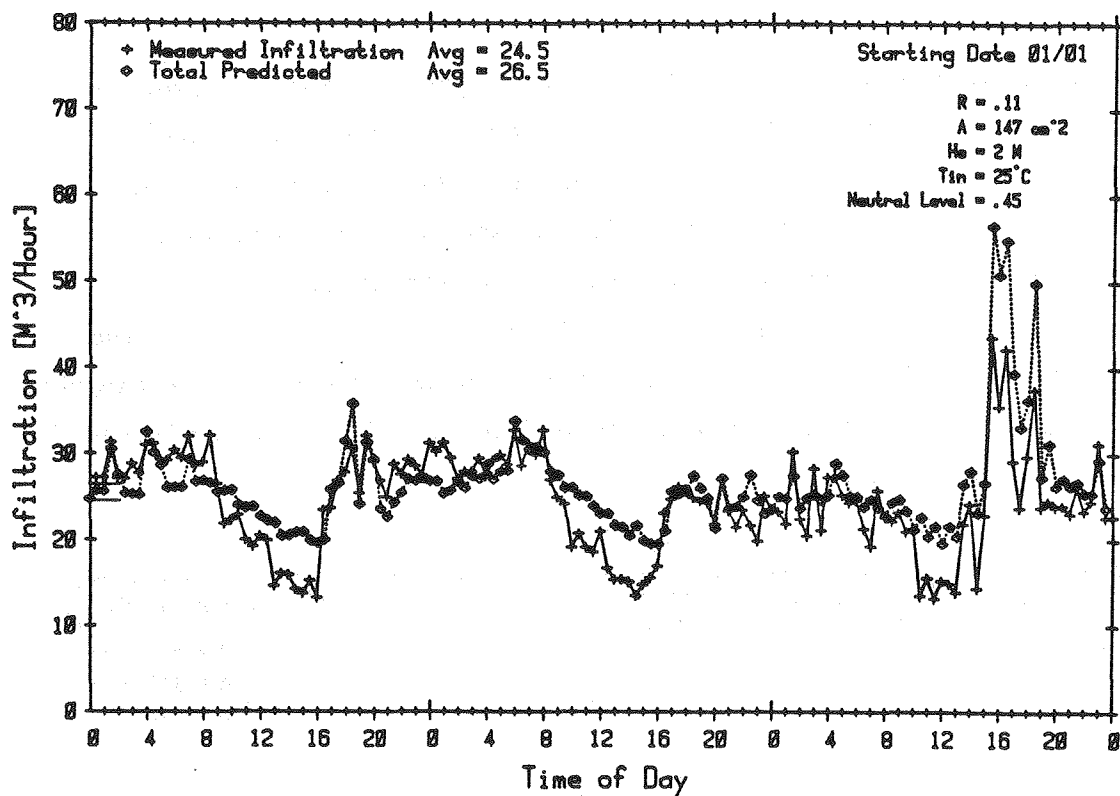


Fig.2 Air Infiltration vs. Time 81/01/01 - 81/01/03. The solid line show measured infiltration values; the dotted line shows values predicted for the MITU using Eq (3).

Application of the Infiltration Model to Residential Audits

The infiltration model is applied in residential energy audits organized on three different levels. We describe each audit briefly followed by the procedures used for infiltration calculations. The first is a residential audit procedure that uses field measurements to assess the current condition of a house. The values obtained in the measurements are used as inputs to a microprocessor to compute the house's energy load. After calculating the energy load, the microprocessor examines a list of retrofits that can be applied to this structure and produces a list of retrofits, rank-ordered by their cost effectiveness.

The Microprocessor-based Energy Audit

Before the actual audit visit, past utility bills of the house and weather data are screened to obtain an "energy signature" for the house. Subsequently, two auditors visit the house. They note window types and measure dimensions, test the envelope for leakage with a blower door that pressurizes or depressurizes the house, identify leaks, plug the easy ones as they go and note the ones that are more difficult to repair. While one auditor measures furnace efficiency, checks water and air-temperature settings, and estimates envelope R-values, the other auditor repairs air leaks, installs water-heater insulation, changes the furnace air filter, calibrates the thermostat and, with the permission of the homeowner, installs a low-flow showerhead and resets the water-heater thermostat.

At the conclusion of the physical inspection, all necessary data are collected and fed to the microprocessor. The microprocessor features a state-of-the-art interactive program that asks simple questions and provides further information on its questions when requested. The homeowner is present during this process and is encouraged to answer the questions either directly or through the auditors. The auditors then help the homeowner decide on a suitable retrofit package. The program scans a master retrofit list stored on a disk that includes conservation measures, such as insulation, storm and double-pane windows, insulating shutters, caulking and weatherstripping, vent dampers, replacement burners, and active and passive solar retrofits for space and water heating.

There is ample occasion for interaction between the homeowner and the program to insure that no optimized retrofit lists are produced with items unacceptable to the homeowner, and that the homeowner is educated on-site about the costs and benefits of retrofits. Of course, our cost estimates of all retrofit packages acknowledge that homeowners may do some retrofits themselves and hire a contractor to do others. At the conclusion of the visit, the auditor leaves behind specific detailed information on the suggested retrofits.

Use of Infiltration Model in the Instrumented Audit -- The Reference House

On the basis of our infiltration model, we have developed a procedure simple enough to be used by auditors with relatively little technical training. In this application we use the concept of a reference house in reference surroundings. The reference house is a single-story building (height = 2.5m) with average leakage distribution ($R = 0.5$; i.e., ceiling and floor leakage areas together are equal to the wall leakage area). By reference surroundings we mean terrain class III (rural areas with low buildings and trees) and shielding class III (some obstructions within two house heights).

It is useful at this point to introduce the term specific infiltration, which is the infiltration divided by the leakage area, L . To obtain numerical values of convenient size, the units used for infiltration are m^3/hr while those for effective leakage area are cm^2 . Referring to Eq (3) we see that the stack component of the specific infiltration is $f_s (\Delta T)^{1/2}$ while the wind component is $f_w v$. During the audit it is the effective leakage area that is measured. If auditors know the value of the specific infiltration for a reference house for that location, they need only multiply the specific infiltration by the measured ELA to find the infiltration required.

We have calculated monthly values of specific infiltration for the reference house in reference surroundings for 59 cities, using weather tapes for Test Reference Years (TRY-tapes). Table 3 shows seasonal averages (November through March) of wind and stack components as well as total specific infiltration.

It is interesting to note that the variation in infiltration per-unit-leakage area across the U.S. is relatively small for this reference case. Fifty percent of the specific infiltration values for the stack and wind components are within ± 0.025 of the median values of 0.17 and 0.22 [m³/hr/cm²], respectively. The total specific infiltration displays a similar stability across the U.S. Fifty percent of the values are within ± 0.03 of the median value of 0.28 [m³/hr/cm²].

Although field measurements of infiltration rates in different houses show significant variation, Table 3 shows comparatively little variation of infiltration rates across the country. The apparent contradiction is resolved when we consider that 1) all of our infiltration figures are expressed per-unit-leakage area and actual houses have leakage areas varying by a factor of three or more; 2) we used a reference house situated in reference surroundings for all calculations. For houses or surroundings different from the reference case (height = 2.5m, R = 0.5, terrain class = III and shielding class = III), we must apply the appropriate corrections, as described below.

Corrections for Non-reference Cases

For houses or surroundings different from the reference case, we apply appropriate corrections by means of the following equations:

$$\frac{Q_{\text{stack}}^{\text{act}}}{L} = cf_s \frac{Q_{\text{stack}}^{\text{ref}}}{L} \quad (8.1)$$

$$\frac{Q_{\text{wind}}^{\text{act}}}{L} = cf_w \frac{Q_{\text{wind}}^{\text{ref}}}{L} \quad (8.2)$$

where: act refers to the actual values,
 ref refers to the values for the reference case,
 cf_s is the correction factor for the stack term,
 cf_w is the correction factor for the wind term.

The correction factors have been computed from Eq. (7) and (8) and are given

Table 3: Seasonal specific infiltration ($\text{m}^3/\text{hr}/\text{cm}^2$) in 59 U.S. cities							
City	$\frac{Q_{\text{stack}}}{L}$	$\frac{Q_{\text{wind}}}{L}$	$\frac{Q}{L}$	City	$\frac{Q_{\text{stack}}}{L}$	$\frac{Q_{\text{wind}}}{L}$	$\frac{Q}{L}$
Albany, NY	.21	.23	.31	Medford OR	.18	.10	.21
Albuquerque	.18	.17	.24	Memphis TN	.15	.21	.26
Amarillo TX	.17	.30	.35	Miami FL	.00	.20	.20
Atlanta GA	.15	.22	.26	Minneapolis	.23	.23	.32
Bismarck ND	.24	.23	.33	Nashville TN	.16	.22	.27
Boise ID	.19	.20	.27	New Orleans	.12	.22	.25
Boston MA	.19	.32	.37	New York NY	.17	.27	.32
Brownsville	.05	.26	.27	Norfolk VA	.15	.26	.31
Buffalo NY	.20	.29	.35	Oklahoma Ci.	.17	.32	.36
Burlington	.21	.22	.31	Omaha NE	.20	.23	.31
Charleston	.13	.21	.25	Philadelphia	.18	.26	.32
Cheyenne WY	.20	.29	.35	Phoenix AZ	.12	.10	.16
Chicago IL	.19	.22	.29	Pittsburgh	.19	.19	.27
Cincinnati	.18	.20	.27	Raleigh NC	.16	.21	.26
Cleveland OH	.20	.25	.32	Richmond VA	.18	.19	.26
Columbia MO	.18	.22	.29	Sacramento	.16	.14	.21
Detroit MI	.20	.26	.33	Salt Lake C.	.20	.18	.27
Dodge City	.19	.29	.35	San Antonio	.12	.21	.25
El Paso TX	.15	.19	.24	San Diego CA	.11	.15	.19
Fort Worth	.14	.25	.29	S. Francisco	.14	.19	.24
Fresno CA	.14	.12	.19	Seattle WA	.17	.22	.28
Great Falls	.21	.36	.42	St. Louis MO	.19	.24	.30
Houston TX	.12	.25	.27	Tampa FL	.06	.21	.21
Indianapol	.19	.24	.31	Tulsa OK	.16	.24	.29
Kansas City	.19	.23	.30	Washing. DC	.17	.17	.24
Lake Charles	.12	.21	.24	Jacksonville	.10	.20	.23
Los Angeles	.11	.17	.20	Jackson MS	.14	.22	.26
Louisville	.18	.23	.29	Portland ME	.21	.19	.28
Lubbock TX	.16	.30	.34	Portland OR	.17	.23	.29
Madison WI	.21	.21	.30				

explicitly below:

$$cf_s = 0.506 (1 + R/2) \left[1 - \frac{X^2}{(2-R)^2} \right]^{3/2} \sqrt{H_h} \quad (9.1)$$

$$cf_w = 8.15 \alpha_h (H_h/10)^{\gamma_h} C' (1 - R)^{1/3} \quad (9.2)$$

where: R is the actual fractional horizontal leakage area,
 X is the actual fractional difference in horizontal leakage area,
 H_h is the height of the house,
 α_h γ_h are the actual terrain class constants for the house, and
 C' is the actual shielding coefficient.

Graphical Techniques for Finding Infiltration

During the audit described above, leakage areas are computed using the microprocessor. A second class of audit uses instrumentation for measurement but computes energy loads in a less sophisticated way. For this latter case we have devised a graphical technique that can be used easily when computers or calculators are not present. Fig. 3 shows a juxtaposition of the calibration curve for the blower door we use and a pressure-flow graph that can be used to construct the flow characteristic of the house we are measuring. During a field pressurization test, the auditor notes the RPM of the fan at several specific pressure differences, then converts these RPM readings to air-flow readings with the help of the fan calibration curves traced in the left half of the figure. In the right half, each measured point, with its pressure difference as the abscissa and the corresponding air flow as the ordinate, is plotted. Since the axes are both logarithmic, the points should lie approximately along a straight line. The best-fitting straight line is extrapolated to 4 pascals and yields the leakage area of the house.

Two sample curves are traced in Fig. 3: the upper set of points was measured in a house before retrofit; the lower half was measured after six hours of sealing leaks, caulking cracks and inserting gaskets in electrical fixtures. The leakage area decreased from 1,250 cm² to 625 cm². This 50% reduction will cause a corresponding decrease in infiltration.

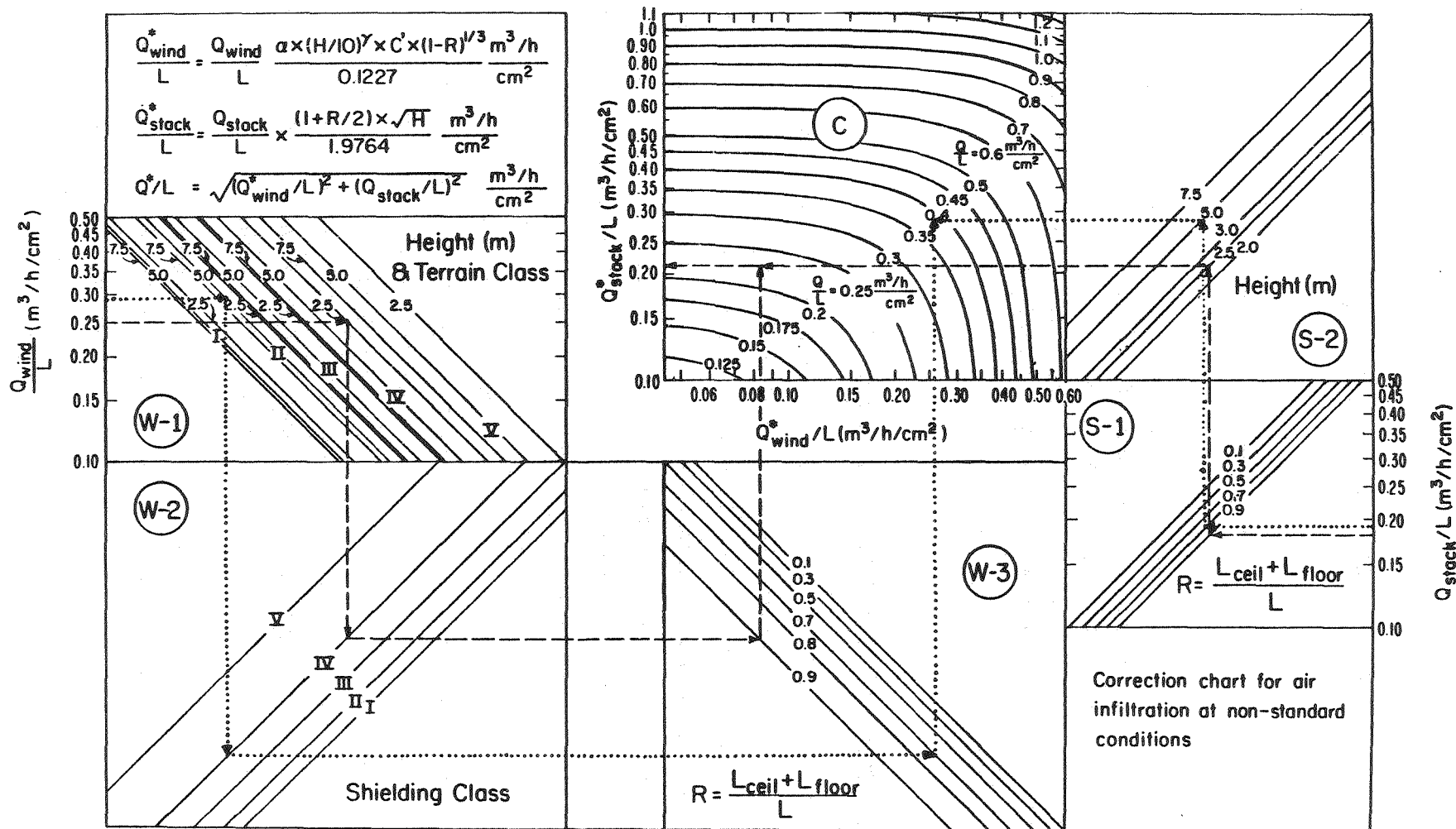


Fig.4 Correction chart for air infiltration at non-standard conditions.

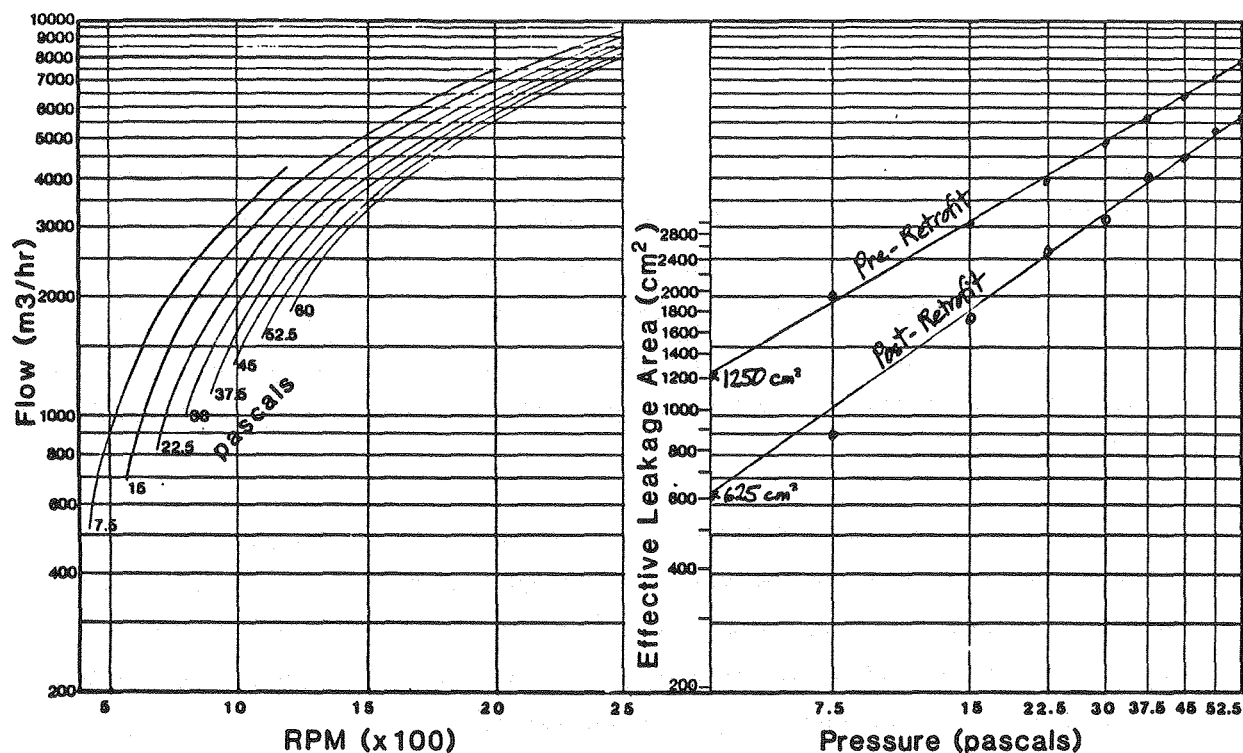


Fig.3 Nomograph to find the effective leakage area of the house from the calibration curve of the blower door.

Corrections for Non-reference Cases -- Graphical Techniques

Corrections for non-reference conditions are effected using Fig. 4. Suppose that we wanted to find the seasonal infiltration of a two-story farm house ($H_h = 5.0\text{m}$) in the middle of wheat fields near Dodge City, Kansas. Let us assume that the house is surrounded by tall trees and that, due to its age, it has an unusually large number of cracks in the ceiling and in the floor. By consulting Tables 1 and 2, we find that terrain class II and shielding class IV best describe the surroundings of this house. The above-normal floor and ceiling leakage area means an R of about 0.7. Table 3 tells us that for reference conditions in Dodge City we should expect a stack-driven infiltration term of $0.19 \text{ m}^3/\text{hr}/\text{cm}^2$ and a wind-driven term of $0.29 \text{ m}^3/\text{hr}/\text{cm}^2$.

Fig. 4 allows corrections for non-reference cases to be applied graphically. The corrections to the wind-driven infiltration are applied by starting at the upper left-hand side of the figure and tracing through quadrants W-1 through W-3. Starting from the value of 0.29 on the left scale of W-1 we

draw a horizontal dotted line to the diagonal line representing terrain class II and height 5m. At this point we drop a dotted line vertically downward into quadrant W-2 to intersect the line marking Shielding Class IV. Next, the dotted line is drawn horizontally into quadrant W-3 until it intersects with the line representing $R = 0.7$. Proceeding vertically upward, the bottom scale of quadrant C gives the corrected value of the wind component of the infiltration, $0.26 \text{ m}^3/\text{hr}/\text{cm}^2$.

The stack-driven infiltration is corrected by starting at the lower right-hand side of Fig. 4 and tracing through quadrants S-1 and S-2. Drawing a dotted line horizontally from the uncorrected value of stack-driven infiltration of 0.19 to the value of $R = 0.7$ in quadrant S-1, then vertically into quadrant S-2 to the height 5 m, then horizontally to the left border of S-2 gives a corrected value of the stack component of the infiltration of $0.29 \text{ m}^3/\text{hr}/\text{cm}^2$. The intersection, in quadrant C, of the wind and stack lines originating in quadrants W-3 and S-2 determines the combined infiltration rate of $0.39 \text{ m}^3/\text{hr}/\text{cm}^2$.

The spacing of the correction lines in Fig. 4 graphically illustrates the importance of individual parameters affecting infiltration. For example, the relatively narrow distance in quadrant S-1 between the lines with highest and lowest R indicates that the stack-driven infiltration is not greatly affected by variations in the leakage distribution. Meanwhile, shielding class and terrain class have great influence on the infiltration rate, as seen in quadrants W-1 and W-2. In the example treated above, it was the increase in height of the structure (5m compared to 2.5m in the reference case) that was the primary cause of the increase in infiltration for the reference case from 0.35 to $0.39 \text{ m}^3/\text{hr}/\text{cm}^2$. The change in terrain class was largely compensated by the change in shielding.

Note that in our graphical corrections we have not considered the difference between ceiling and floor leakage area (described by the parameter $X = (L_{\text{ceiling}} - L_{\text{floor}})/L$). We have assumed this parameter to be always zero (that is, ceiling and floor leakage areas were assumed to be equal). As indicated by the detailed equations presented above, our results are relatively insensitive to this parameter -- thus its omission in the corrections.

Application to a Walk-through Audit

In most audits, neither microprocessors nor fan pressurization equipment will be available. Consequently, the infiltration portion of the audit will be a visual inspection of the structure followed by an estimate of current average infiltration.

Again the LBL infiltration model is an ideal basis for constructing an infiltration estimation procedure. The technique currently employed in the model Residential Conservation Service audit was developed using an earlier version of the model [9] and is described below.

The leakage area is estimated by examining eight different groups of building features. Each group contributes approximately equal amounts to the total leakage area of the structure. The auditor notes the condition of each feature (good, average or poor) following the guidelines of Table 4, below. The sum of the number of categories rated "good" is multiplied by one, those rated "average" by two, and the sum rated "poor" by three. The total of the three values is normalized by dividing by eight (the total number of categories) to produce a leakage factor, N, having a value between one and three.

The infiltration is

$$Q = A_F N v f \quad (10)$$

where: Q is the infiltration [m^3/hr],
A_F is the floor area of the living space [m^2],
N is the leakage factor described above,
v is the average wind speed for the area [km/hr], and
f is a shielding factor.

The shielding factor, f, has the value of .05 for shielded sites (shielding class IV of Table 2), 0.10 for average sites (shielding class III), and 0.15 for exposed sites (shielding class II).

Table 4 Component Leakage Guidelines

	BUILDING COMPONENT	GOOD	AVERAGE	POOR
[1]	WINDOWS AND DOORS	<input type="checkbox"/> WINDOW AND DOOR FRAMES CAULKED. WINDOW AND DOOR SASHES WELL FITTING AND WEATHER-STRIPPED OR STORM WINDOWS AND DOORS WITH GOOD FIT.	<input type="checkbox"/> WINDOW AND DOOR FRAMES CAULKED OR WINDOW AND DOOR SASHES WEATHERSTRIPPED OR POORLY FITTING STORM DOORS AND WINDOWS.	<input type="checkbox"/> NO CAULKING ON WINDOW AND DOOR FRAMES. NO WEATHER-STRIPPING. NO STORM DOORS OR WINDOWS
[2]	WALLS AND ELECTRICAL OUTLETS	<input type="checkbox"/> CEILING AND FLOOR JOINTS AND CORNERS WELL SEALED. ELECTRICAL OUTLETS WITH GASKETS. NO HOLES AROUND PLUMBING PENETRATIONS.	<input type="checkbox"/> SOME CRACKS IN CEILING AND FLOOR JOINTS AND CORNERS. NO GASKETS ON ELECTRICAL OUTLETS. LESS THAN THREE PLUMBING PENETRATIONS WITH HOLES AROUND THEM.	<input type="checkbox"/> MANY CRACKS IN CEILING AND FLOOR JOINTS AND CORNERS. NO GASKETS ON ELECTRICAL OUTLETS. THREE OR MORE PLUMBING PENETRATIONS WITH HOLES AROUND THEM.
[3]	ATTIC FLOOR (CEILING)	<input type="checkbox"/> NO CRACKS IN ATTIC FLOOR. NO AIR SHAFTS AROUND FLUES. NO HOLES AROUND DUCTS, PIPES OR WIRING PENETRATING ATTIC FLOOR. NO RECESSED LIGHT FIXTURES. NO TRAP DOOR OR WEATHERSTRIPPED TRAP DOOR TO ATTIC.	<input type="checkbox"/> SOME CRACKS IN ATTIC FLOOR. NO AIR SHAFTS AROUND FLUES. SOME HOLES AROUND DUCTS, PIPES OR WIRING PENETRATING ATTIC FLOOR. LESS THAN THREE RECESSED LIGHT FIXTURES. UNWEATHERSTRIPPED TRAP DOOR TO ATTIC	<input type="checkbox"/> MANY CRACKS IN ATTIC FLOOR. AIR SHAFTS AROUND FLUES. HOLE AROUND DUCTS, PIPES OR WIRING PENETRATING ATTIC FLOOR. MORE THAN THREE RECESSED LIGHT FIXTURES. UNCOVERED ATTIC ACCESS.
[4]	HEATING SYSTEM & WATER HEATER	<input type="checkbox"/> BOTH FURNACE AND WATER HEATER ELECTRIC. IF FOSSIL FUEL-FIRED. BOTH IN UNCONDITIONED SPACE.	<input type="checkbox"/> ONE FOSSIL FUEL-FIRED UNIT IN LIVING SPACE WITH VENT DAMPER. THE OTHER IN UNCONDITIONED SPACE.	<input type="checkbox"/> AT LEAST ONE FOSSIL FUEL-FIRED UNIT IN LIVING SPACE WITHOUT VENT DAMPER.
[5]	FIREPLACE OR WOOD STOVE	<input type="checkbox"/> SEALED COMBUSTION WOOD STOVE OR FIREPLACE WITH WELL FITTING DAMPER AND GLASS DOORS OR NO FIREPLACE.	<input type="checkbox"/> POORLY SEALED WOOD STOVE OR FIREPLACE WITH EITHER WELL FITTING DAMPER OR GLASS DOORS.	<input type="checkbox"/> BOTH A WOOD STOVE AND FIREPLACE OR A FIREPLACE WITH POORLY FITTING DAMPER AND NO GLASS DOORS.
[6]	DUCTWORK AND FLOOR	<input type="checkbox"/> NO DUCTWORK AND FEW FLOOR PENETRATIONS OR ALL DUCTWORK IN CONDITIONED SPACE AND NO FLOOR PENETRATIONS.	<input type="checkbox"/> DUCTWORK IN CONDITIONED BASEMENT AND FEW FLOOR PENETRATIONS.	<input type="checkbox"/> DUCTWORK IN UNCONDITIONED SPACE AND MANY FLOOR PENETRATIONS.
[7]	VENTS IN CONDITIONED SPACE	<input type="checkbox"/> NO UNDAMPED VENTS AND LESS THAN THREE DAMPERED VENTS.	<input type="checkbox"/> LESS THAN THREE UNDAMPED VENTS OR AT LEAST THREE DAMPERED VENTS.	<input type="checkbox"/> MORE THAN THREE UNDAMPED VENTS.
[8]	LIFESTYLE	<input type="checkbox"/> LESS THAN SIX ENTRANCES AND EXITS PER DAY.	<input type="checkbox"/> SIX TO THIRTEEN ENTRANCES AND EXITS PER DAY.	<input type="checkbox"/> MORE THAN THIRTEEN ENTRANCES AND EXITS PER DAY.
[9]	TOTALS	<input type="checkbox"/> +	<input type="checkbox"/> +	<input type="checkbox"/> = 8

The Problem of Retrofits

There is a lengthy list of retrofit options available that reduce air leakage in buildings. The auditor is faced with the problem of selecting the most effective retrofits from this list to recommend to homeowners. For this application, the results of the infiltration model are again instructive. It predicts that, on average, a change in the infiltration of the structure is proportional to the change in the total leakage area. Unfortunately, field measurements of the leakage area of various building components or the changes in leakage area associated with various retrofit procedures are limited. At

present, the best summary is the unpublished report of Born and Harrje [10]; however, there are some useful constraints that can be employed to estimate quickly the importance of various leakage sites.

The total leakage area of many houses in the United States and Canada has been measured in several different studies [11-13]. For purposes of exploring these data, we have found it useful to use the concept of specific leakage area (SLA) to organize data. The SLA is defined as the ratio of the effective leakage area of a house (measured in units of centimeters squared) to the house's floor area (measured in units of meters squared). Using the concept of SLA eliminates differences in the ELA of similar houses due solely to variations in the size of the house. The choice of units used for the SLA yields values of SLA in the range of 1 to 20 [cm^2/m^2], a convenient range when analyzing large groups of data. Fig. 5 shows box plots* of the SLA of several groups of houses measured recently. Box plots of the average infiltration of the same group of houses (for the period from 1 November through 31 March) are shown in Fig. 6.

A comparison of Fig. 5 and 6 emphasizes the importance of the specific leakage area in determining the average infiltration of similar structures.

The basic difference between Fig. 5 and 6 are the average weather conditions that drive infiltration at the various locations. The remarkable similarity between Fig. 5 and 6 reflect the stability of the average weather conditions that drive infiltration, an observation noted earlier in discussing Table 3.

Clearly, the component leakage values we are interested in determining must be consistent with the total leakage areas measured in the studies referred to above.

An example of the reduction in leakage area that may be obtained in a careful audit procedure, including patching major leakage sites, is presented in the box plot shown in Fig. 7. This plot shows the reduction in total

* A box plot, a useful way to represent a large group of data, was introduced by Tukey [14]. The two extreme values of the data are represented by circles, the extremes of the box represent the values separating the first and second quartiles, and the third and fourth quartiles; while the line through the center of the box represents the median value to the data set.

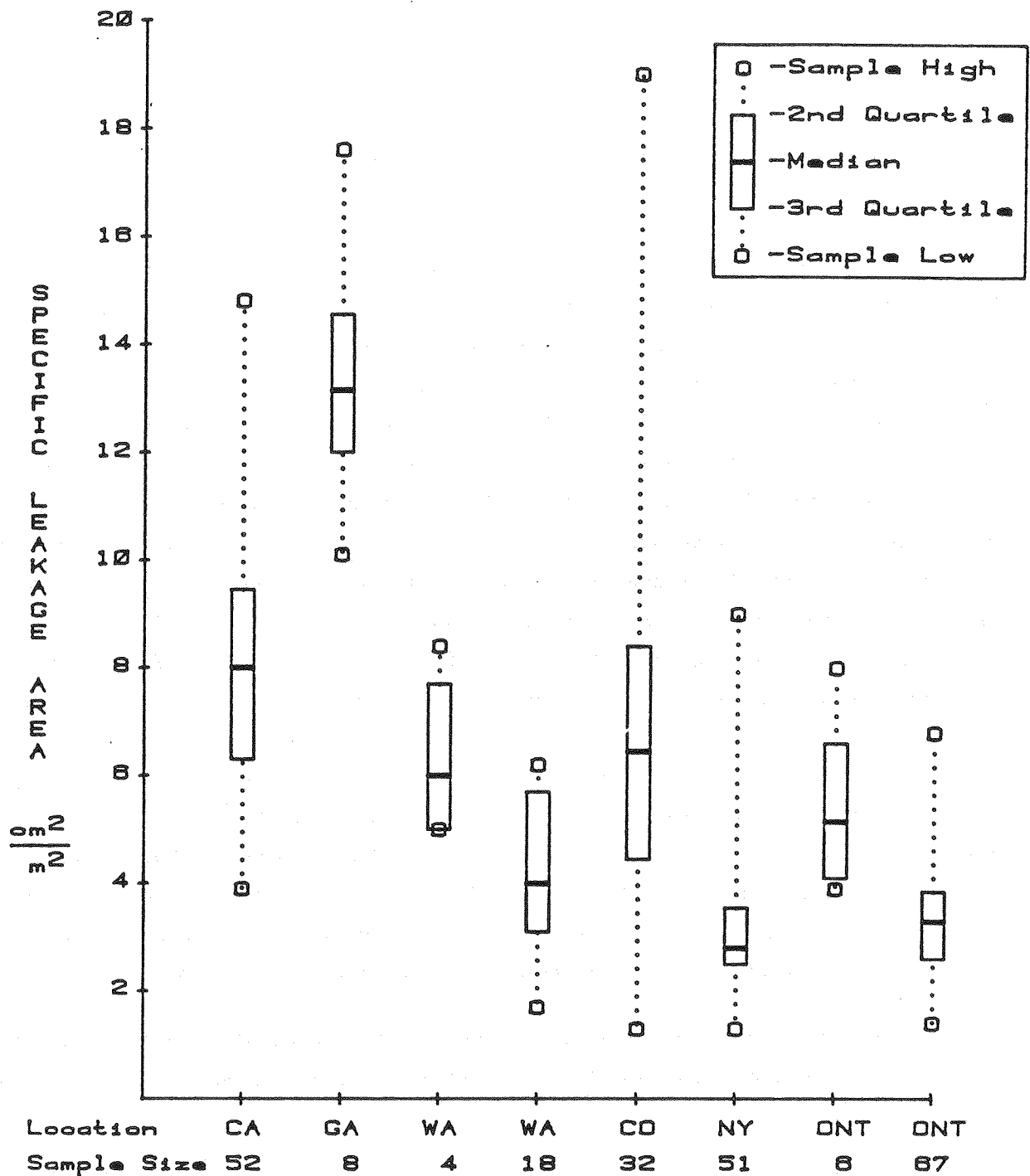
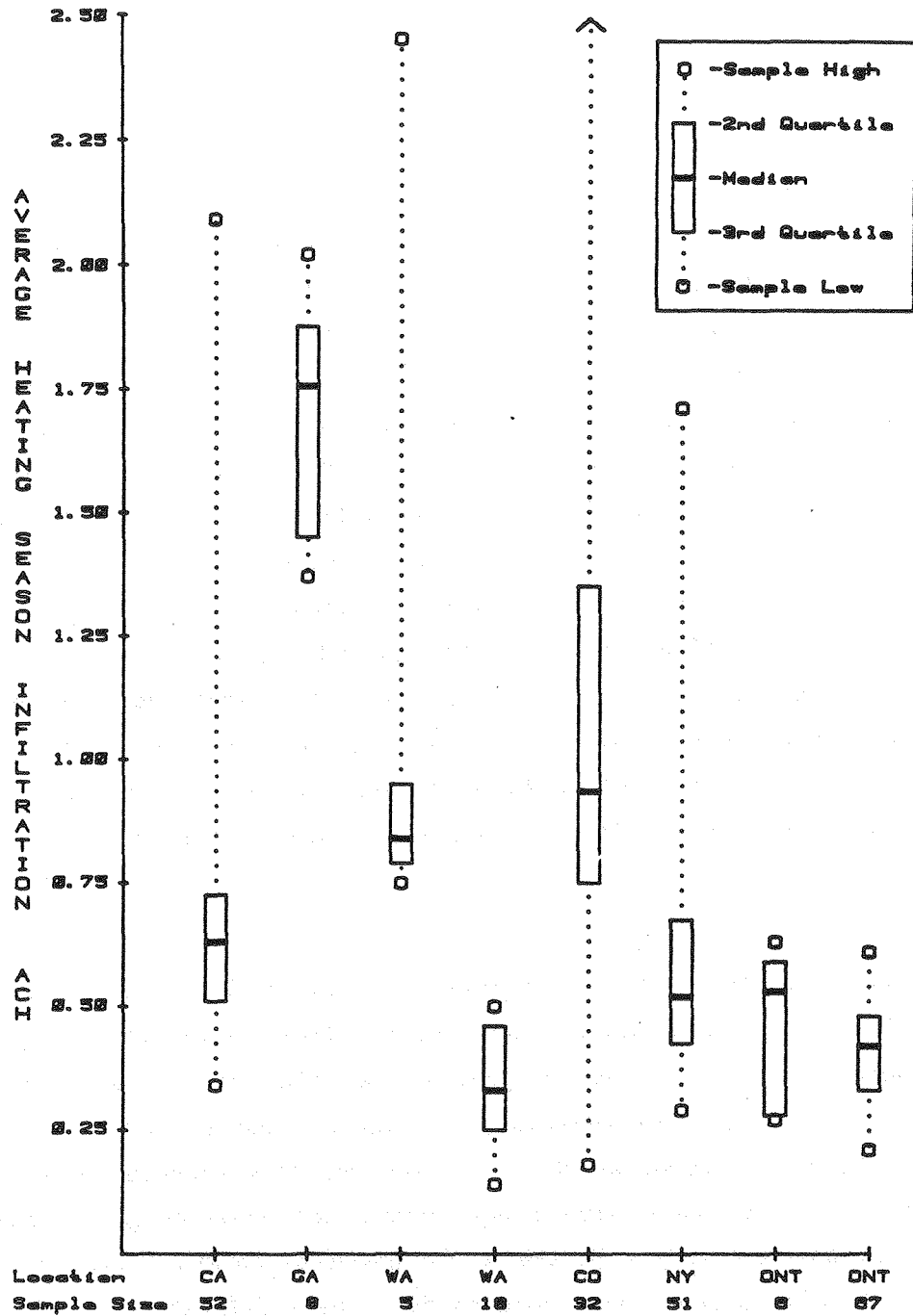


Fig.5 Specific leakage areas of groups of houses measured in North America. The number of degree days for each location increases to the right.

leakage area obtained by two auditors working in large single-family residences in Walnut Creek, CA for a single day.



HEATING SEASON (NOVEMBER-MARCH) INFILTRATION RATES

Fig.6 Average infiltration for the Nov.-March heating season for the houses shown in Fig.5. These are values calculated from the model described in this report.

Fig. 7 shows that the median SLA decreased from 8.6 to 6.0 cm^2/m^2 , a reduction of 29%. The minimum change obtained in the 16-house sample was 14%, the maximum, 65%.

An example illustrating the lack of effectiveness in reducing air infiltration of a standard "add insulation and storm windows" retrofit is shown in Fig. 8 [12]. Eighteen houses owned by Bonneville Power Administration are included in the study. The sample was divided into three groups or "cells" during the first phase of the project. Cell 1 was a control group; cell 2 received only attic insulation, and cell 3 received attic insulation, crawl-space insulation and storm windows. The left box of each set is the mid-quartile range of the specific leakage area before retrofit; the right gives results of measurements nine months after retrofit.

In no case in Fig. 8 did the median SLA of a group decrease. Preliminary sampling of energy use after the retrofits showed 13% reduction for group 2 and 29% reduction in group 3. A second phase of the project includes retrofits to reduce air leakage, the sampling of indoor air quality before and after retrofit, and the installation of mechanical ventilation systems with air-to-air heat exchangers to assure adequate ventilation and heat recovery.

CONCLUSIONS

To summarize, infiltration measurements in the context of an instrumented energy audit can be made quickly and accurately by using the fan pressurization technique. The measurement provides a value of the effective leakage area of the structure. In addition, particular leakage sites can easily be identified by using smoke sticks or other air-flow-pattern detectors. The technique is direct, uses simple equipment, and provides measurement values that can be analyzed simply in the field using computers, calculators or the graphical techniques described above to find the infiltration.

In an uninstrumented "walk-through" audit the results of the infiltration model can be used to generate a prescription for estimating seasonal infiltration. Both techniques focus on the idea of the leakage area, the parameter that most characterizes the infiltration of a structure. This parameter, when normalized by dividing by the floor area of the building, is a useful measure of the infiltration performance of groups of buildings in retrofit projects.

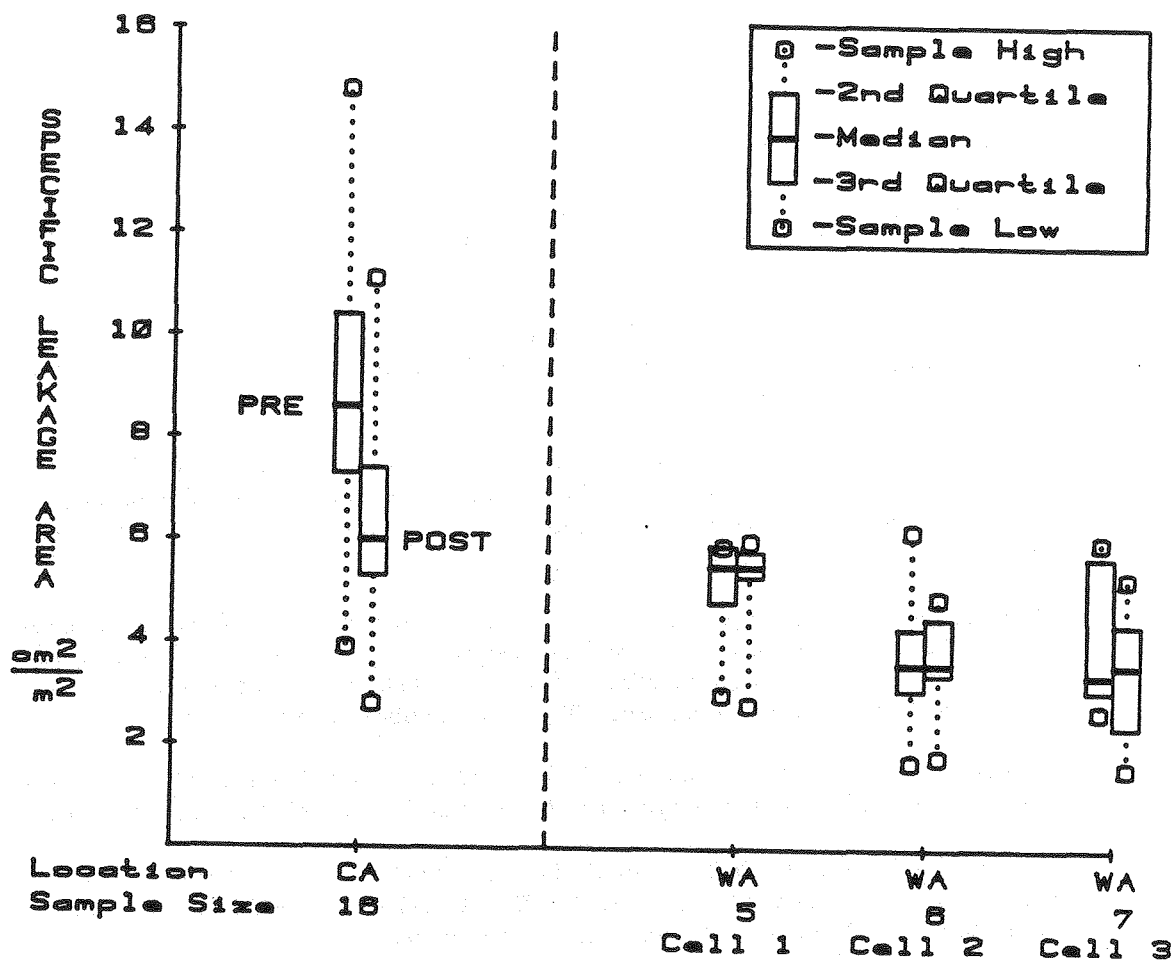


Fig.7 Specific leakage areas for pre- and post-retrofit conditions in a House-Doctor demonstration in Walnut Creek, CA.

Fig.8 Pre- and post-retrofit measurements of specific leakage areas in three groups of houses in phase I of BPA energy conservation project.

References

1. Hitchin, E.R., and Wilson, C.B. 1967. "A Review of Experimental Techniques for the Investigation of Natural Ventilation in Buildings." Building Science 2: 59-82.
2. Hunt, C.M. 1980. "Air Infiltration: A Review of Some Existing Measurement Techniques and Data." In Building Air Change Rate and Infiltration Measurements, ASTM STP 719, ed. C.M. Hunt, J.C. King, and H.R. Trechsel, pp. 3-23. Philadelphia: American Society for Testing Materials.
3. Sherman, M.H., Grimsrud, D.T., Condon, P.E., and Smith, B.V. 1981. "Air Infiltration Measurement Techniques." Proceedings of the 1st Air Infiltration Centre Conference "Air Infiltration Instrumentation and Measurement Techniques" Windsor, UK, 6-8 October 1980.
4. Kronvall, J., 1978. "Testing of Houses for Air-Leakage Using a Pressure

Method." ASHRAE Trans. 84: 72-79.

5. Blomsterberg, A.K., and Harrje, D.T. 1979. "Approaches to Evaluation of Air Infiltration Energy Losses in Buildings." ASHRAE Trans. 85: 797-815.
6. Grimsrud, D.T., Sherman, M.H., and Diamond, R.C. 1979. "Infiltration-Pressurization Correlations: Detailed Measurements on a California House." ASHRAE Trans. 85: 851-865.
7. Sherman, M.H., Grimsrud, D.T., and Sonderegger, R.C. 1979. "The Low Pressure Leakage Function of a Building." Proceedings of the ASHRAE/DOE Conf. "Thermal Performance of the Exterior Envelopes of Buildings" 3-5 December.
8. Sherman, M.H., and Grimsrud, D.T. 1981. "Measurement of Infiltration Using Fan Pressurization and Weather Data." Proceedings of the 1st Air Infiltration Centre Conference "Air Infiltration Instrumentation and Measuring Techniques" Windsor, UK, 6-8 October 1980.
9. Sherman, M.H., and Grimsrud, D.T. 1980. "Infiltration-Pressurization Correlation: Simplified Physical Modeling." ASHRAE Trans. 86: 778-807.
10. Born, G. and Harrje, D.T. 1980. "Review and Interpretation of Air Infiltration in Residential Housing." Unpublished Note from the Center for Environmental Studies, Princeton University.
11. Tamura, G. 1975. "Measurement of Air Leakage Characteristics of House Enclosures." ASHRAE Trans. 81: 202-208.
12. Krinkel, D.L., Dickerhoff, D.J., Casey, J.S., and Grimsrud, D.T. 1980. "Pressurization Test Results: Bonneville Power Administration Energy Conservation Study." Lawrence Berkeley Laboratory Report No. LBL-10996.
13. Beach, R.K. 1979. "Relative Tightness of New Housing in the Ottawa Area." Division of Building Research, National Research Council of Canada building research note no. 149.
14. Tukey, J.W. 1977. Exploratory Data Analysis. Reading, Mass: Addison-Wesley.